Bioelectrochemistry 146 (2022) 108128

Contents lists available at ScienceDirect

Bioelectrochemistry

journal homepage: www.journals.elsevier.com/bioelectrochemistry

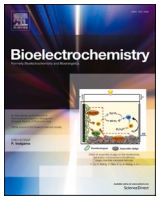

A biophotoelectrode based on boronic acid-modified *Chlorella vulgaris* cells integrated within a redox polymer☆

Zaida Herrero-Medina [a], Panpan Wang [b], Anna Lielpetere [b], Abdulaziz S. Bashammakh [c], Abdulrahman O. Alyoubi [c], Ioanis Katakis [a,*], Felipe Conzuelo [d,*], Wolfgang Schuhmann [b,*]

[a] *Departament d' Enginyeria Química, Universitat Rovira i Virgili, Av. Països Catalans 26, 43007 Tarragona, Spain*
[b] *Analytical Chemistry - Center for Electrochemical Sciences (CES), Faculty of Chemistry and Biochemistry, Ruhr University Bochum, Universitätsstr. 150, D-44780 Bochum, Germany*
[c] *Department of Chemistry, King Abdulaziz University, 21589 Jeddah, Saudi Arabia*
[d] *Instituto de Tecnologia Química e Biológica António Xavier, Universidade Nova de Lisboa, Av. da República, 2780-157 Oeiras, Portugal*

ARTICLE INFO

Keywords:
Biophotovoltaics
Boronic acid
Redox polymers
Chlorella vulgaris
Photocurrent

ABSTRACT

Green microalgae are gaining attention in the renewable energy field due to their ability to convert light into energy in biophotovoltaic (BPV) cells. The poor exogenous electron transfer kinetics of such microorganisms requires the use of redox mediators to improve the performance of related biodevices. Redox polymers are advantageous in the development of subcellular-based BPV devices by providing an improved electron transfer while simultaneously serving as immobilization matrix. However, these surface-confined redox mediators have been rarely used in microorganism-based BPVs. Since electron transfer relies on the proximity between cells and the redox centres at the polymer matrix, the development of molecularly tailored surfaces is of great significance to fabricate more efficient BPV cells. We propose a bioanode integrating *Chlorella vulgaris* embedded in an Os complex-modified redox polymer. *Chlorella vulgaris* cells are functionalized with 3-aminophenylboronic acid that exhibits high affinity to saccharides in the cell wall as a basis for an improved integration with the redox polymer. Maximum photocurrents of (5 ± 1) μA cm^{-2} are achieved. The developed bioanode is further coupled to a bilirubin oxidase-based biocathode for a proof-of-concept BPV cell. The obtained results encourage the optimization of electron-transfer pathways toward the development of advanced microalgae-based biophotovoltaic devices.

1. Introduction

Chlorella vulgaris (*C. vulgaris*) is a green microalgae widely used in pharmaceutical and nutraceutical industries [1-4] with great potential as a renewable energy source as feedstock for biofuel cells [5-7] or through direct light-to-energy conversion in biophotovoltaic (BPV) cells [8-11]. BPV cells are a promising green energy technology since they use photosynthetic microorganisms [8-10,12] or subcellular photosynthetic apparatus, i.e., thylakoid membranes, chloroplasts, or even isolated photosystems [13,14], enabling to harnessing solar light and generate electricity using only water as electron source.

One of the most important factors limiting the performance of microorganism-based BPVs is the cell-to-electrode electron transfer (ET). Ideally, more environmentally friendly, cost-effective and long-lasting BPV devices could be achieved based on direct electron transfer (DET) [15,16] between cells and the electrode through redox proteins or pili-like structures on the cell wall surface as in the case for electrogenic bacteria in microbial fuel cells (MFCs) [17,18]. However, DET remains elusive for a great majority of microorganisms. Thus, the use of electron mediators that boost the ET kinetics has become necessary [19]. Among these, surface-confined redox mediators such as Os-complex-modified redox polymers (P-Os) have shown to be promising materials to electronically communicate with photosynthetic microorganisms [20-22]. P-Os forms a 3D-hydrogel that can integrate the microorganisms, facilitating their immobilization and the electron transfer to the electrode by electron hopping between adjacent Os-complexes [23,24]. Higher and faster ET rates can be achieved if stronger interactions that direct the redox centres to be in proximity with

☆ Dedicated to Prof. Frieder Scheller on the occasion of his 80th birthday.

* Corresponding authors.
E-mail addresses: ioanis.katakis@urv.cat (I. Katakis), felipe.conzuelo@itqb.unl.pt (F. Conzuelo), wolfgang.schuhmann@rub.de (W. Schuhmann).

https://doi.org/10.1016/j.bioelechem.2022.108128
Received 13 February 2022; Received in revised form 22 March 2022; Accepted 29 March 2022
Available online 5 April 2022

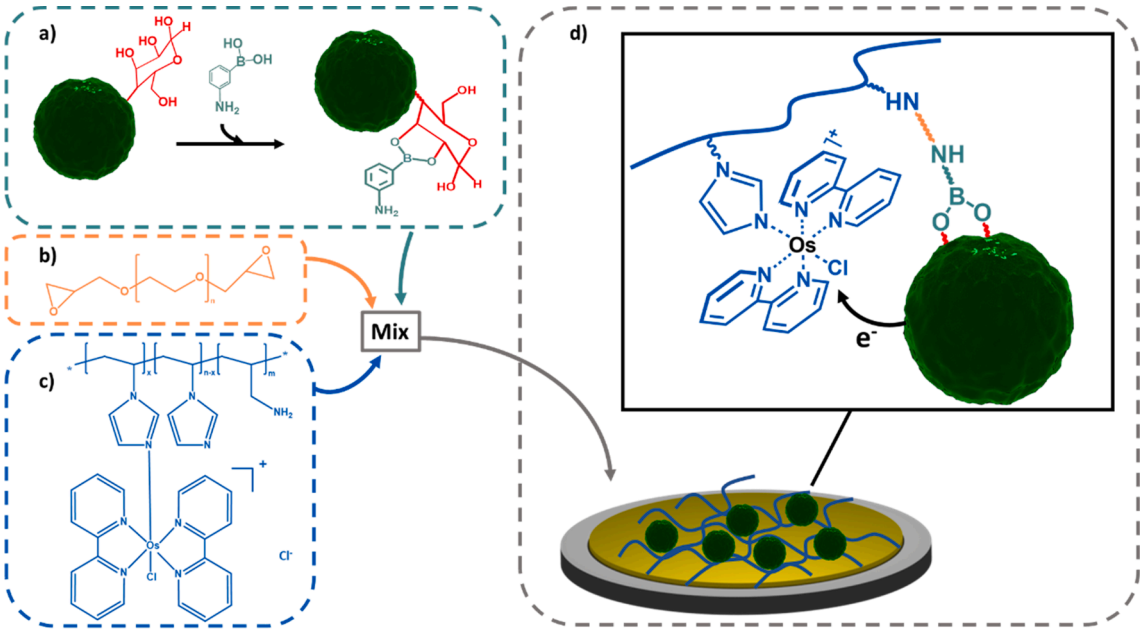

Fig. 1. (a) Schematic of covalent binding of 3-APBA with polysaccharides on the cell wall of *Chlorella vulgaris* during the preincubation step. Chemical structures of (b) poly(ethylene glycol) diglycidyl ether (PEGDGE) and (c) poly(1-vinylimidazole-*co*-allylamine)-[Os(2,2′-bipyridine)$_2$Cl]Cl (P-Os). (d) Schematic of the bioanode: gold electrode modified with *C. vulgaris* with covalently bound 3-APBA embedded within a P-Os hydrogel matrix crosslinked with PEGDGE. Inset: proposed crosslinking of amino groups of both P-Os and 3-APBA bound to cells.

phototrophs immobilized within the hydrogel matrix can be attained. In this regard, boronic acid derivatives have been used to electronically communicate cells to electrode surfaces for cytosensing purposes [25,26] and in MFCs [27] by covalent binding to 1,2- and 1,3-*cis*-diols of saccharides present in the cell wall and cellular membranes. More recently, poly-(3-aminophenylboronic acid) has successfully been employed to improve the photoelectrogenesis of *C. vulgaris* [28].

In this work, we report an improved electronic communication between an Os-complex modified redox polymer and boronic acid modified *C. vulgaris* cells. 3-aminophenylboronic acid (3-APBA) is incorporated to increase the intimate contact between the redox polymer and the immobilized cells, thus improving the integration of *C. vulgaris* with the polymer redox centers and enhancing the stability of the resulting biofilm. Furthermore, as a proof of concept, the proposed bioanode is coupled to a bilirubin oxidase biocathode to build a BPV cell.

2. Materials and methods

2.1. Cell culture

The *C. vulgaris* strain 211-11b was purchased from Sammlung von Algenkulturen der Universität Göttingen (SAG). Cultures were grown in 100 mL of Bold's basal medium (BBM) [29] in 250 mL Corning polycarbonate Erlenmeyer flasks (Fisher Scientific) at (20 ± 2) °C and 150 rpm with an irradiance of ≈ 50 μmol photons m^{-2} s^{-1} on a 12 h light:12 h dark regime.

2.2. Anode modification

When cultures reached the exponential phase, they were centrifuged at 4 °C and 4000 rpm for 10 min, washed in 0.1 M phosphate buffer (PB) pH 7, centrifuged again and concentrated in a fresh solution of 2 mg mL^{-1} 3-APBA in 0.1 M PB pH 7 until an optical density at 680 nm (OD_{680}) of 5 was achieved (cuvette of 1 cm optical path length). The resuspended culture with 3-APBA was kept under agitation at 200 rpm for 2 h at room temperature (RT). Afterwards, it was ultra-filtrated with Vivaspin 500, 10,000 MWCO (Sartorius) tubes to remove the loosely bound 3-APBA and resuspended in 0.1 M PB pH 7 to a final OD_{680} of 10. Prior to modification, gold disk electrodes of 2 mm Ø (CH Instruments) were polished with diamond slurries of 0.1 μm (LECO) and subsequently ultrasonicated in ethanol and deionized water for 5 min. Afterwards, the electrodes were electrochemically cleaned in 0.5 M H_2SO_4 for 10 cycles at 0.1 V s^{-1} from −0.2 V to 1.6 V vs. Ag/AgCl/3 M KCl. Au-coated wafers prepared as reported in [30] were cleaned with Piranha solution and rinsed with deionized water prior to modification. Afterwards, 3 μL of a freshly prepared solution consisting of 1.7 mg mL^{-1} of the redox polymer poly(1-vinylimidazole-*co*-allylamine)-[Os(bpy)$_2$Cl]Cl (P-Os, synthesized as described in [31]), 0.033 mg mL^{-1} of poly (ethylene glycol) diglycidyl ether (PEGDGE, Mn = 400 g mol^{-1}, Polysciences), and 6.25 OD mL^{-1} of *C. vulgaris* were drop-cast on the electrode and desiccated for 3 h at 21 °C and 10% relative humidity (RH). Next, the hydrogel was collapsed by dipping the electrode for 30 min in Tris-HCl buffer (AppliChem) pH 9 containing 10 mM $CaCl_2$, 10 mM $MgCl_2$ and 100 mM KCl, and was left to dry.

2.3. Electrochemical analysis of the anode:

All electrochemical measurements were performed in a three-electrode electrochemical cell with the modified gold electrode, Pt wire and Ag/AgCl/3 M KCl as the working, counter, and reference electrodes, respectively. All potentials are referred vs. Ag/AgCl/3 M KCl. To assess the anode performance, cyclic voltammetry (CV) at a scan rate of 10 mV s^{-1} and chronoamperometry (CA) were performed using a PalmSens2 potentiostat (Palmsens) in 0.1 M PB, pH 7 and at an irradiation of 50 mW cm^{-2} of white light supplied by a He-Xe lamp (LC8 type 03, Hamamatsu photonics). The applied potential for the CA was 350 mV, which ensures the oxidation of the P-Os, allowing the collection of electrons coming from the immobilized cells.

To evaluate the action spectrum, the modified Au-electrodes with and without *C. vulgaris* cells were polarized to 350 mV with an Autolab PGSTAT302N (Methrom Autolab) under irradiation cycles of 20 s. Each irradiation cycle was performed at different wavelengths ranging from 297 nm to 797 nm selected by a monochromator setup (Instytut Fotonwy) placed immediately in front of a 150 W Xe lamp (Ushio) used

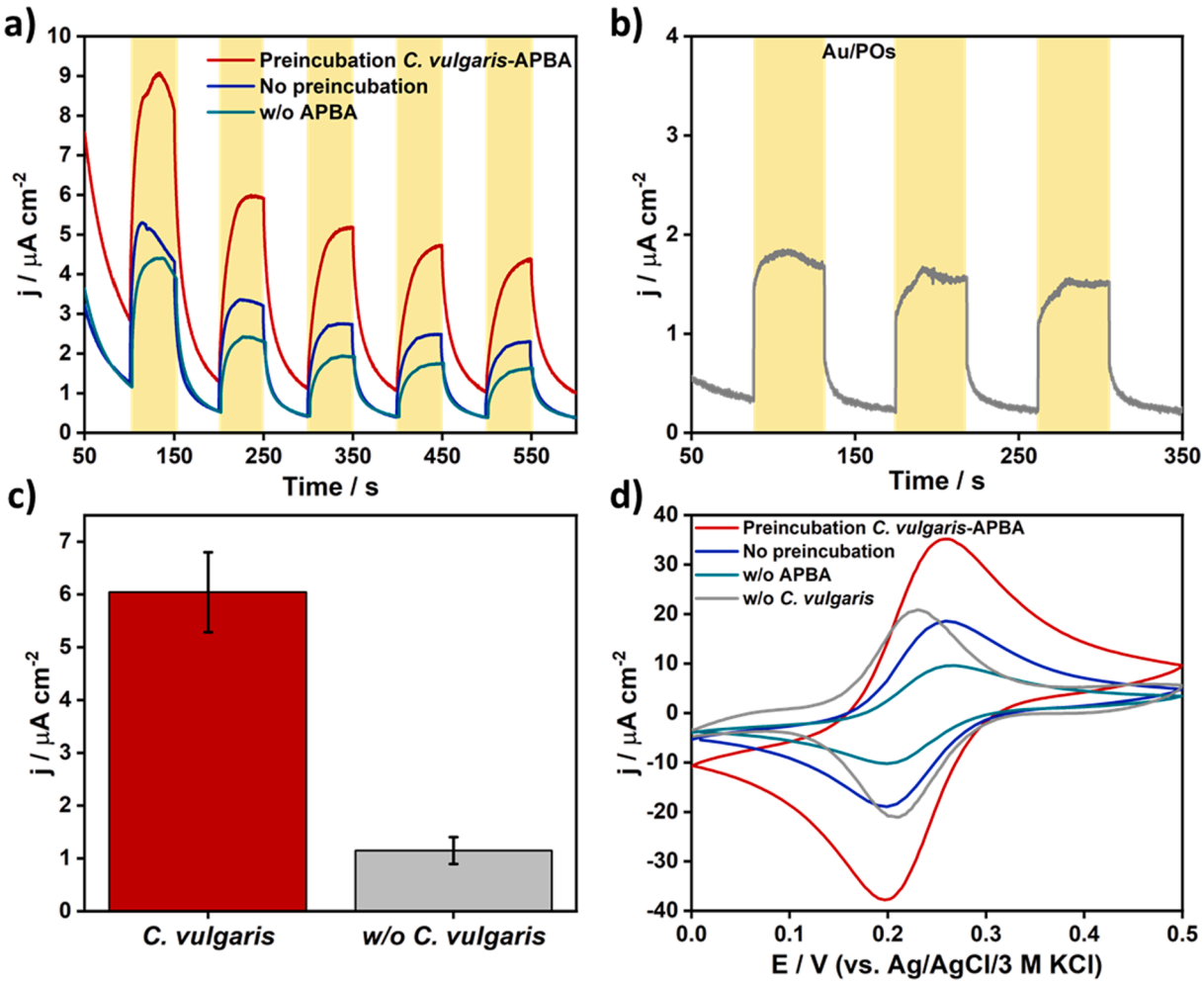

Fig. 2. (a) CA of electrodes modified with P-Os integrating *Chlorella vulgaris* cells preincubated with 3-APBA (red line), P-Os with *C. vulgaris* and 3-APBA directly mixed without preincubation (blue line), and P-Os integrating *C. vulgaris* in the absence of 3-APBA (green line). (b) CA of P-Os modified electrode without *C. vulgaris* (grey line). E_{app} = 350 mV vs. Ag/AgCl/3 M KCl. Irradiation with 50 mW cm^{-2} incident white light (yellow shadows). (c) Comparison of the average responses for P-Os modified electrodes in the absence and presence of *C. vulgaris* (n = 3). Error bars represent the standard deviation. (d) CV recorded for electrodes after CA as shown in (a) and (b). Scan rate: 10 mV s^{-1}. Electrolyte: 0.1 M PB buffer, pH 7.

as light source. The photocurrent at each wavelength was normalized to the photon flux at each wavelength.

2.4. Chlorophyll a (Chl a) UV–Vis spectroscopy:

Extraction of Chl *a* from *C. vulgaris* was performed following a method adapted from [32] under subdued light. Briefly, cultures were centrifuged at 4 °C and 5000 rpm for 10 min, washed with 0.1 M PB pH 7 and the pellet was resuspended in the same buffer. Then, pellets were lyophilized and resuspended in pure methanol (Sigma-Aldrich) (pre-treated with magnesium carbonate to remove any acid) and kept at 4 °C for 4 h. Then 0.1 mm zirconia beads were added, and the cells were disrupted by means of MiniBead Beater-8 (Biospec) for 1 min. Afterwards, the cultures were centrifuged, the pellet was discarded and the spectrum of the supernatant (Chl *a*) was measured from 350 nm to 800 nm in quartz cuvettes with an UV–Vis spectrophotometer Cary 100 Bio (Varian).

2.5. DCMU and DCBQ experiments:

Solutions of 10 mM of the photosynthetic inhibitor 3-(3,4-dichlorophenyl)-1,1-dimethylurea (DCMU, Sigma-Aldrich) and 10 mM of the redox mediator 2,6-dichloro-1,4-benzoquinone (DCBQ, Sigma-Aldrich) dissolved in pure ethanol (Sigma-Aldrich) were prepared for being used at the final concentrations as further specified in the *Results and discussion* section.

2.6. Scanning photoelectrochemical microscopy (SPECM):

SPECM measurements were performed with the *C. vulgaris*-based bioanode as the sample interrogated by the SPECM tip. The electrochemical cell was filled with 0.1 M PB, pH 7, and the bioanode, a Pt mesh and a Ag/AgCl/ 3 M KCl were the working (sample electrode), the counter and reference electrodes, respectively. The tip was a Pt disk microelectrode (25 µm Ø Pt wire, Goodfellow). Full details of the SPECM setup are described elsewhere [33]. Local illumination of the sample with white light was attained by coupling the lamp with the top glass of the tip microelectrode by means of a light fiber (HITRONIC POF Simplex PE). Photochronoamperometry was performed with the tip microelectrode positioned at one tip radius distance above the sample surface. The sample was polarized to 350 mV and the tip microelectrode was poised to −600 mV for the reduction of O_2.

2.7. Preparation and characterization of the biocathode:

Prior to modification, graphite electrodes of 3 mm Ø (SGL Carbon) were polished with sandpaper and then rinsed with deionized water. Then, the electrodes were modified by oxidation of 2-aminobenzoic acid

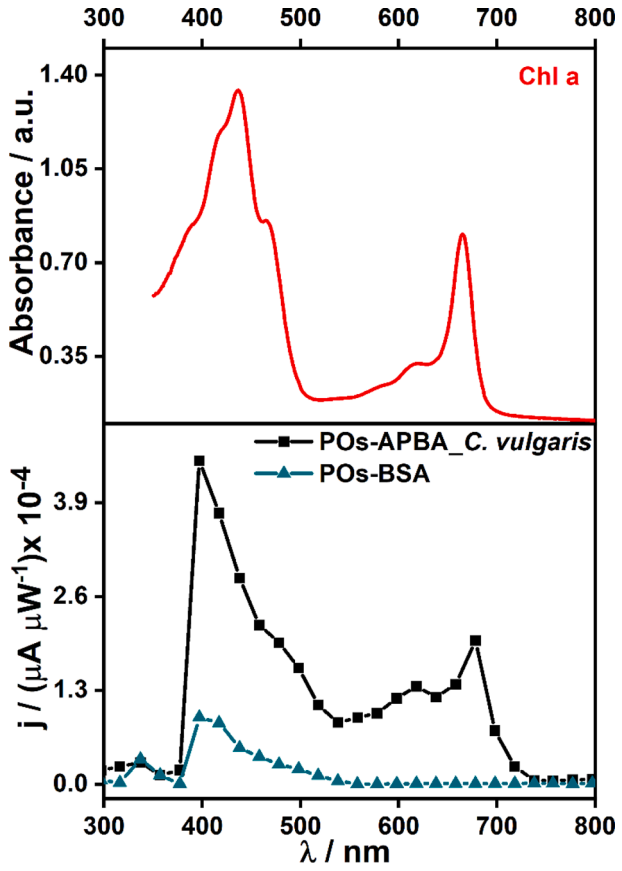

Fig. 3. Comparison of the absorption spectrum of chlorophyll *a* (Chl *a*) extracted from *Chlorella vulgaris* (top) and the action spectra of P-Os modified electrodes (bottom) integrating either BSA (green) or *C. vulgaris* (black). E_{app} = 350 mV vs. Ag/AgCl/3 M KCl. Electrolyte: 0.1 M PB buffer, pH 7.

(2-ABA) (Sigma-Aldrich) in 0.1 M KCl solution at 0.8 V for 60 s as described elsewhere [34]. Subsequently, the modified electrodes were rinsed with deionized water to remove loosely bound 2-ABA and shortly dried at RT. 20 μL of a solution of 5 mg mL^{-1} of *Myrothecium verrucaria* bilirubin oxidase (*Mv*-BOD) (Sigma-Aldrich) in 0.1 M phosphate buffer saline (PBS) (Sigma-Aldrich) pH 7 were drop-cast on the electrode surface and allowed to dry at RT. Afterwards, the electrodes were washed with deionized water to remove loosely bound enzyme. *Mv*-BOD-modified electrodes were characterized by CV from 0.6 V to 0 V at a scan rate of 10 mV s^{-1} in 0.1 M PBS pH 7 in both air and Ar atmosphere.

2.8. Biophotovoltaic measurements:

A single chamber BPV cell was constructed by coupling the *C. vulgaris*-modified photoanode with the *Mv*-BOD biocathode. The electrolyte solution was 0.1 M PB pH 7. The bioanode surface with an area of 0.636 cm^{-2} was exposed to white light with an incident power of ≈ 200 mW cm^{-2}. Polarization and power curves were calculated by measuring the steady-state current in dark and light conditions at different applied cell voltages using a PGU-BI 100 potentiostat (IPS Jaissle).

3. Results and discussion

C. vulgaris-based bioanodes were constructed by modifying a gold electrode surface with *C. vulgaris* cells embedded within a P-Os hydrogel matrix crosslinked with PEGDGE. Prior to the integration of the microalgae in the hydrogel, *C. vulgaris* cells were functionalized with 3-APBA, which covalently binds to 1,2 and 1,3 *cis*-diols of saccharides present in the cell wall, in order to improve the crosslinking between the P-Os and the cells. Although it is not expected to be a quantitative reaction, the ring-opening of the epoxide by the substituted aniline without catalyst in water is expected [35-37] (Fig. 1). Similarly to previously reported enzyme and photosystem-modified bioelectrodes, the use of PEGDGE during electrode modification assists in the formation of a more stable film over the electrode as a highly cross-linked matrix can be obtained [31,38].

The maximum photocurrent ((6.0 ± 0.7) μA cm^{-2}) was obtained for this bioanode during the first illumination cycle and it decayed to almost half after the fifth cycle of illumination (Fig. 2a). To investigate the role of 3-APBA in enhancing the intimate contact and thus contributing to an improved electronic communication between microalgae and the redox polymer, the photochronoamperometric performance of the *C. vulgaris*-based bioanode was compared with P-Os modified electrodes in the absence of *C. vulgaris*. After subtracting the photocurrent arising from photoexcitation of the redox polymer alone (Fig. 2b), the average net photocurrent for *C. vulgaris* was (5 ± 1) μA cm^{-2} (Fig. 2c). This photocurrent is almost 10 times higher than that obtained in previous reports (0.64 μA cm^{-2}) with *C. vulgaris* immobilized within an alginate matrix [10] and more than two times higher than the maximum reported so far (2.0 ± 0.6 μA cm^{-2}) with *C. vulgaris* immobilized on poly(3-aminophenylboronic acid)-modified electrodes [28]. In addition, control experiments were performed by fabricating biophotoelectrodes with a mixture of cells and 3-APBA but without a preincubation step and without 3-APBA (Fig. 2a). In contrast to the optimized bioanode, lower photocurrents (about 33% lower) were obtained when the cells were directly mixed with P-Os and 3-APBA before drop-casting (i.e., without preincubation with 3-APBA). These lower photocurrents might be due to a shorter time for interaction preventing the formation of covalent bonds between the boronic acid moiety in 3-APBA and polysaccharides of the cell wall than in the situation when cells are preincubated with 3-APBA. Moreover, when the cells were immobilized in the absence of boronic acid, the photocurrent response was also lower and less stable (see Table S1).

CVs in dark conditions recorded after photochronoamperometry for electrodes integrating *C. vulgaris* within the redox hydrogel showed larger peak-to-peak separations for the redox peaks associated with the $Os^{2+/3+}$ interconversion than those for electrodes without the microalgae (see Fig. 2d and Table S2). This indicated the successful incorporation of *C. vulgaris* into the hydrogel matrix, with the cells hampering to some extent the electron-transfer kinetics between the Os-centers within the polymer deposited over the electrode [10]. In addition, higher anodic and cathodic peak currents were also obtained when the cells were preincubated with 3-APBA while the controls using cells without preincubation and without 3-APBA delivered similar or lower peak currents in comparison with P-Os alone (Table S2). These results support our hypothesis that 3-APBA favours the covalent attachment of amino moieties of P-Os *via* PEGDGE crosslinking [25] to the amino groups of 3-APBA at the cell wall. Supposedly, this crosslinking is contributing to bringing the Os centers in close proximity to the cell wall of *C. vulgaris*, which facilitates the electron transfer from the microalgae via P-Os to the electrode causing increased photocurrent generation (Fig. 2a and c).

To demonstrate that the origin of the photocurrent is due to the presence of *C. vulgaris* and that the Os complex-modified polymer is responsible for the electron transfer to the electrode, the action spectrum of the bioelectrode was assessed by polarizing the electrode at a constant potential while varying the wavelength at each illumination cycle in the wavelength range from 300 nm to 800 nm. As a control, an electrode with bovine serum albumin (BSA) replacing *C. vulgaris* was used (Fig. S1). BSA is a non-redox active protein able to stabilize the polymer matrix after crosslinking and prevents hydrogel over-swelling leading to a more comparable electron transfer in contrast to electrodes based on P-Os alone [39,40]. Fig. 3 shows that the action spectra profile of redox polymer-modified electrodes with and without *C. vulgaris* are substantially different.

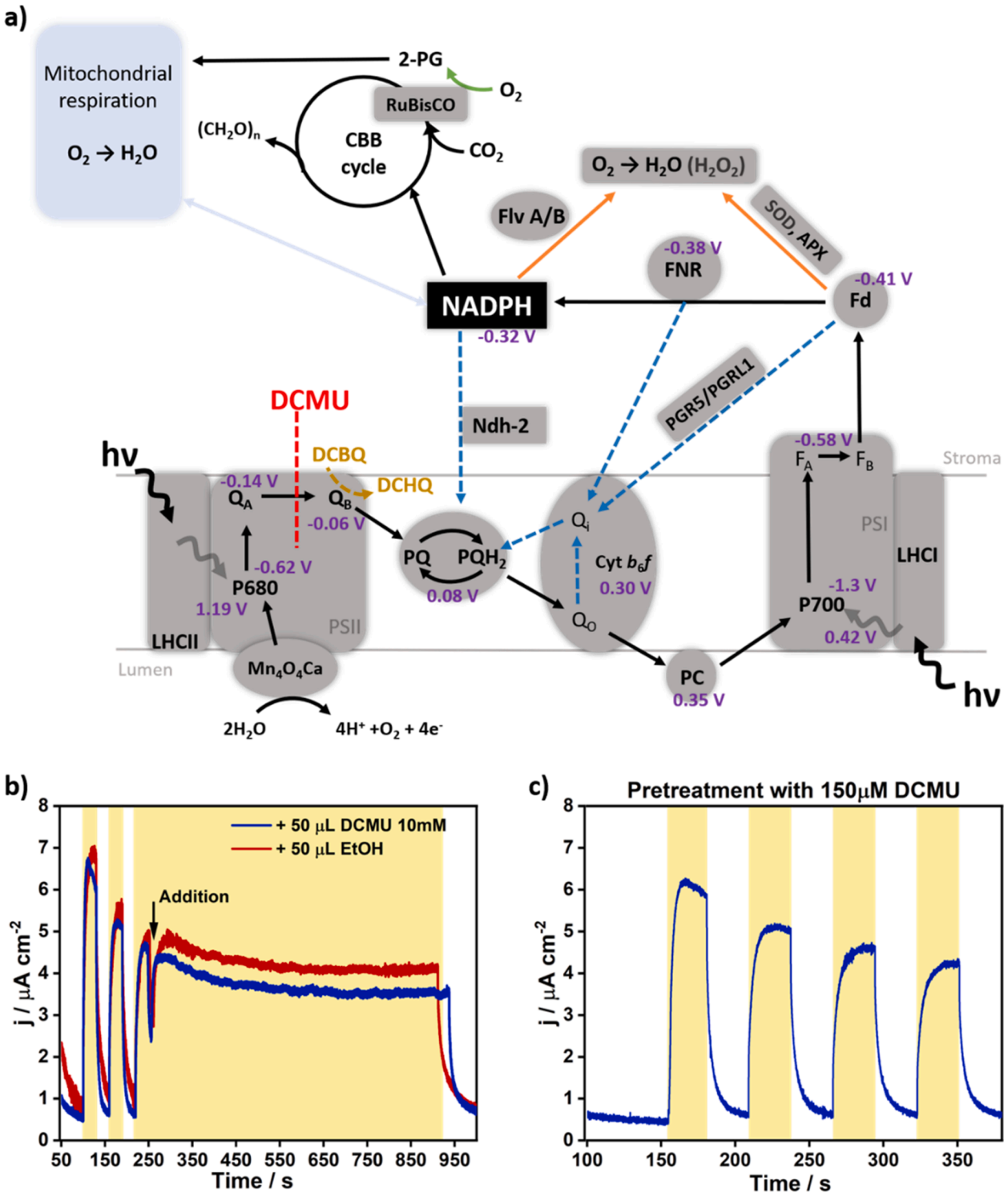

Fig. 4. (a) Schematic of the photosynthetic electron transport chain with the relevant midpoint potentials (V vs. SHE as indicated in [42]). Solid black lines indicate the linear electron transport (LET) from the oxidation of water by photosystem II (PSII) to the reduction of NAPH by Fd-$NADP^+$ reductase (FNR). Putative electron pathways to decrease the over-reduction of the LET during the light phase of the photosynthesis are represented with different colours: cyclic electron transport around photosystem I (PSI) (blue dashed lines), pseudocyclic electron transport or water-water cycle for the photoreduction of O_2 (orange solid lines), photorespiration catalysed by RuBisCO (green solid line), $NAD(P)^+$/NAD(P)H interchange between mitochondria and chloroplast (light blue solid line). APX, ascorbate peroxidase; CBB, Calvin-Benson-Bassham cycle; DCBQ/DCHQ, 2,6-dichloro-1,4-benzoquinoe/hydroquinone; DCMU, 3-(3,4-dichlorophenyl)-1,1-dimethylurea; LHCII/LHCI, light harvesting complexes II and I; Nhd-2, type II NADH dehydrogenase; Fd, ferredoxin; Flv A/B, flavodiiron proteins; PC, plastocyanin; PGR5 and PGRL1, proton gradient regulation 5 and proton gradient regulation like 1; PQ, plastoquinone; SOD, superoxide dismutase. (b) CA of a *C. vulgaris*-based bioanode in presence and absence of DCMU (50 µM) and (c) with pre-treatment of *C. vulgaris* cultures with 150 µM DCMU for 30 min. E_{app} = 350 mV vs. Ag/AgCl/3 M KCl. Electrolyte: 0.1 M PB buffer pH 7. Irradiation with 50 mW cm^{-2} incident white light (yellow shadows).

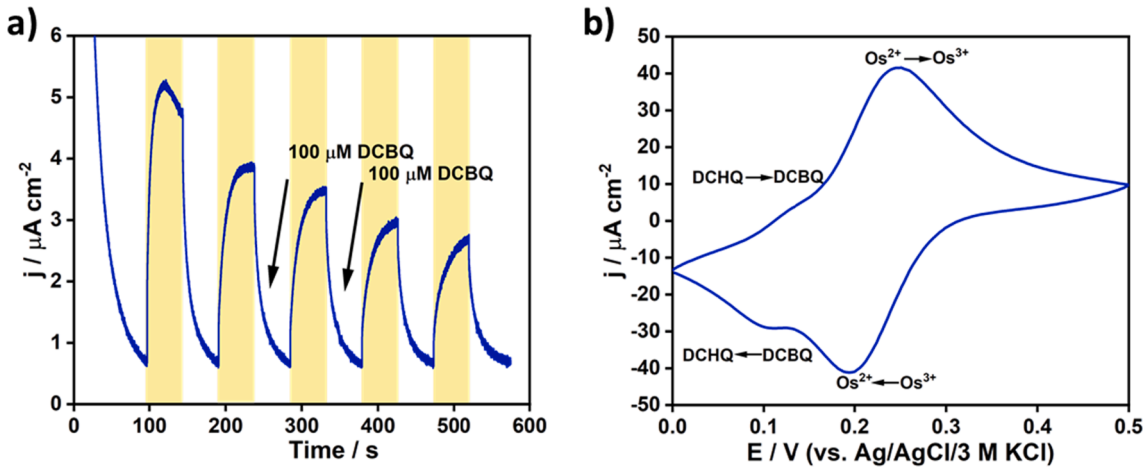

Fig. 5. (a) Chronoamperogram of a *C. vulgaris*-based bioanode with the addition of DCBQ. E_{app} = 350 mV vs. Ag/AgCl/3 M KCl. Irradiation with 50 mW cm^{-2} incident white light (yellow shadows). (b) Cyclic voltammogram after (a) showing the redox peaks for the DCBQ/DCHQ and $Os^{2+/3+}$ interconversions. Electrolyte: 0.1 M PB buffer pH 7.

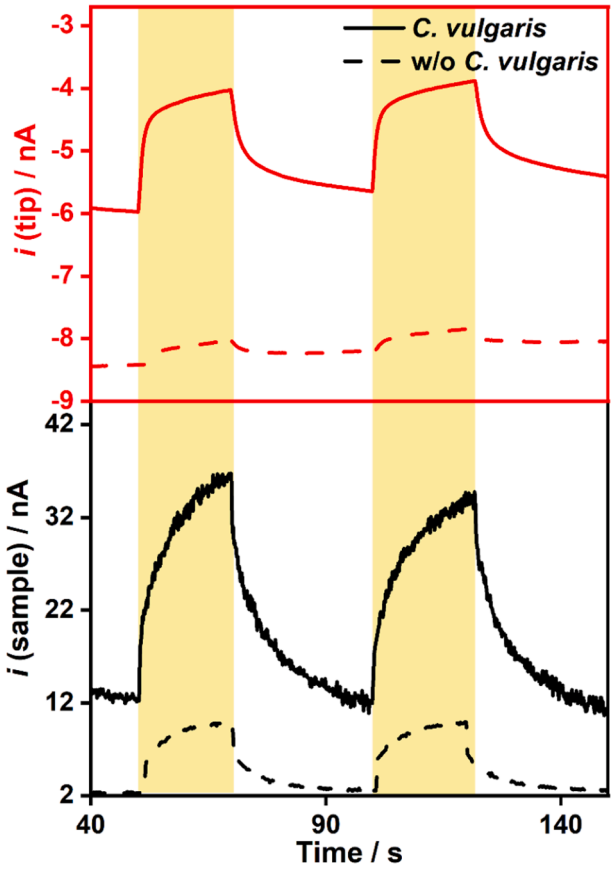

Fig. 6. SPECM analysis of P-Os modified electrodes integrating either BSA (dashed lines) or *Chlorella vulgaris* preincubated with 3-APBA (solid lines). Black: sample photocurrent. Red: tip current for the reduction of O_2. The sample and tip were polarized at 350 mV and −600 mV vs. Ag/AgCl/3 M KCl, respectively. Electrolyte: 0.1 M PB buffer, pH 7. The sample was locally irradiated with ≈ 200 mW cm^{-2}. Tip-to-sample distance: 13 μm.

In the absence of *C. vulgaris* cells, P-Os only exhibits a small photoactivity in the violet to blue wavelength range (from 390 to 520 nm) with a maximum of 0.9 × 10^{-4} μA $μW^{-1}$ at 400 nm. In contrast, when cells are present inside the P-Os film, the photocurrent is up to four times higher than in the absence of cells and the photoresponse persists

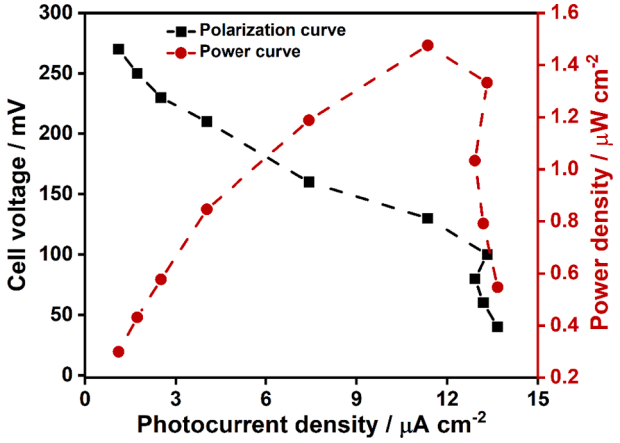

Fig. 7. Polarization (black) and power (red) curves for the assembled BPV cell with a P-Os modified electrode integrating *Chlorella vulgaris* functionalized with 3-APBA as photoanode and a *Mv*-BOD modified electrode as biocathode. The photoanode was irradiated with white light at a power of ≈ 200 mW cm^{-2}. Electrolyte: 0.1 M PB buffer pH 7.

throughout a longer wavelength range (from 390 to 720 nm), with two local maxima of 4.5 × 10^{-4} and 2.0 × 10^{-4} μA $μW^{-1}$ at 400 and 680 nm, respectively. The profile of this action spectrum concurs almost perfectly with the electronic transitions of Chl *a* pigments present in the chloroplasts of *C. vulgaris* as it can be seen in the absorption spectrum of Chl *a*. This strongly supports our hypothesis that photocurrent generation is related with the photosynthetic machinery of *C. vulgaris* and productive electron-transfer communication between the polymer-integrated cells and the electrode via P-Os is established.

To further investigate the source of electrons, the photosynthetic inhibitor DCMU was added to the electrolyte to a final concentration of 50 μM during the third cycle of illumination. DCMU blocks the reduction of the plastoquinone intermediate Q_B by the plastoquinone intermediate Q_A (both located in the photosystem II (PSII) reaction center), preventing further electron transfer to redox proteins of the photosynthetic electron transport chain [41] (Fig. 4a). After the addition of DCMU no significant decrease in photocurrent was observed even after 10 min of illumination, compared to a sample where only the solvent (ethanol) was added (Fig. 4b).

In order to discard the possible impact of 3-APBA and P-Os on the diffusion of DCMU to the immobilized polymer-integrated *C. vulgaris*

Table 1
Comparison of quantum yields calculated with the power reported using photosynthetic elements (subcellular and cellular) as bioanode in biophotoelectrochemical cells:

Photosynth. element	Anode	Cathode	Power output ($\mu W\ cm^{-2}$)	Power input ($mW\ cm^{-2}$)	Quantum yield (%)	Ref.
PSI	Au/P-vio	CC/GOX	3.7	100	3.7×10^{-3}	[53]
PSII	IO-TiO_2/PbS/ P-Os	IO-ATO/PC/ BOD	45	100	45×10^{-2}	[54]
Thylakoid	CP/PFP	MWCNT/ PBSE/ BOD	0.33	100	3.3×10^{-4}	[55]
Thylakoid	ITO/Au/CNT[a]	BOD/KB/WPCC	50	434	1.2×10^{-2}[c]	[56]
Nostoc sp.	CNT/CP [b]	*Laccase*/ CNT/CP	10	76	1.3×10^{-2}	[12]
C. vulgaris	ITO/alginate	ITO	2.6×10^{-3}	2.6	1.1×10^{-4}[c, d]	[10]
C. vulgaris	Au/P-Os	BOD/ Graphite	1.5	200	7.4×10^{-4}	This work

ATO, antimony-tin oxide; GOX, glucose oxidase; IO, inverse opal; ITO, indium-tin oxide; KB/WPCC, ketjen Black-modified waterproof carbon cloth; MWCNT, multiwalled carbon nanotube; PBSE, 1-pyrenebutyric acid N-hydroxysuccinimide ester; PC, pyrenecarboxylic acid; PFP, poly(fluorene-*alt*-phenylene); P-vio, viologen modified polymer.[a and b] used diffusing mediators ruthenium hexaamine trichloride and 1,4-benzoquinone, respectively.[c] calculated from the stated photon flux on the reports converted to power density using Eq. S2. [d] subtracting power output in dark.

cells, a culture of free cells was treated with 150 μM DCMU in 0.1 M PB pH 7 for 30 min prior incubation with 3-APBA and further immobilization with P-Os. Fig. 4c shows that the photocurrent responses were very similar when the cells were exposed to DCMU or using unexposed *C. vulgaris* cells. Moreover, a photochronoamperometric measurement of a *C. vulgaris*-based bioanode was performed in presence of the free-diffusing redox mediator DCBQ after a few irradiation cycles. As shown in Fig. 5a, the addition of DCBQ did not result in an increased photocurrent response meaning that the redox mediator was not reduced to 2,6-dichloro-1,4-hydroquinone (DCHQ) by PSII inside the cells [43] (Fig. 4a). The prevention of the DCBQ electron transfer within the hydrogel could be discarded since an additional pair of redox peaks with a formal potential of 0.11 V vs. Ag/AgCl/3 M KCl for the DCBQ/DCHQ interconversion was observed in the CV of the bioanode (Fig. 5b). All these findings confirm that Q_B is not implicated in photocurrent generation by communication with the redox polymer, and thus, an alternative electron pathway should be involved. As it is unlikely that the redox polymer is able to cross the cell wall and wire the Q_A site at PSII to the electrode as it has been reported for biophotoelectrodes integrating isolated PSII [30,44], the obtained results suggest that there is a source of electrons that interplays downstream of Q_B to eventually be excited by PSI [45].

A closer examination of the mechanism related to the photocurrent generation was performed using SPECM to locally evaluate the oxygen evolution of the system. SPECM has been shown to be a valuable tool for analysing light-reactions at a specific location of the sample, such as oxygen evolution and generation of reactive oxygen species (ROS) by means of microelectrodes polarized at specific potentials [30,46]. In the improbable case of P-Os wiring to Q_A, the oxygen evolution complex (OEC) would be functional, and thus an increase in O_2 collection efficiency associated with the generated photocurrent response would be expected under illumination. Conversely, the obtained SPECM results (Fig. 6) show a considerable decrease in the tip current for O_2 reduction when the sample with immobilized *C. vulgaris* is irradiated, meaning that there is O_2 consumption instead of its production at the analyzed sample under illumination. When the experiment was repeated with a control electrode fabricated with BSA instead of *C. vulgaris*, only a minor (5 times lower) O_2 consumption was observed under illumination, confirming that the observed consumption of O_2 is correlated with the generation of the photocurrent. It is important to note that despite the fact that the photosynthetic and respiratory systems in *Chlorella* are located in separated organelles, there is evidence of cross-talk between them [47-49].

Not only oxygen is consumed by respiration in the mitochondria, but it is also consumed in the chloroplast during the light and dark phases of photosynthesis (chlororespiration, photorespiration, Mehler and Mehler-like reactions) [47,50] as a mechanism to avoid the over-reduction of the photosynthetic machinery under stress conditions (i.e., high light intensity, low concentrations of CO_2 and nutrient starvation) [51,52]. Thus, the oxygen uptake observed in the SPECM might indicate that alternative electron pathways are activated to avoid light photodamage. These results together with the observations from the action spectra (Fig. 3) and the experiments with DCMU and DCBQ (Fig. 4b-c and 5) strongly support our hypothesis that electrons stem from processes downstream of Q_B that involve PSI, whether oxygen is directly involved or not, i.e., cyclic electron transport (CET) (Fig. 4a). To elucidate the exact electron transfer mechanism, further investigation with other inhibitors, mediators and knockout cells should be performed, which is the aim of future research to confirm this hypothesis.

As a proof of concept for a functioning BPV cell, the *C. vulgaris*-based bioanode was coupled to a *Mv*-BOD biocathode. The BPV cell performance was assessed under light and dark regimes (Fig. 7). CVs of the *Mv*-BOD cathode under argon and air were conducted to ensure that the cathode was not limiting the BPV performance (Fig. S2). The open circuit voltage (OCV) of the BPV cell was around 270 mV. After subtracting the background outputs in darkness, a maximum current density of 13.66 $\mu A\ cm^{-2}$ and a power output of 1.48 $\mu W\ cm^{-2}$ at 130 mV were obtained. The quantum yield (QY) of the BPV cell was calculated dividing the power output by the power input (light supply) and compared to quantum yields for previous works of biophotoelectrochemical cells. The quantum yield attained (7.4×10^{-4} %) was lower than the obtained with devices using subcellular elements or cyanobacteria as a bioanode (Table 1), since the electron transfer is hampered due to the presence of biological barriers to surpass. Nevertheless, the quantum yield obtained with our system was greater than other configurations using *C. vulgaris* as a bioanode.

4. Conclusions

A bioanode comprised of *Chlorella vulgaris* cells functionalized with 3-APBA embedded in an Os complex-modified polymer matrix has been developed. The binding of 3-APBA with the cells increases the stability of the resulting film as well as promotes the photocurrent presumably due to an improved crosslinking between the redox polymer matrix and immobilized cells. Furthermore, the overlap between the absorbance spectrum of Chl *a* and the action spectrum of the bioanode, indicates that the photocurrent is mainly due to the photoexcitation of the photosynthetic machinery of the immobilized *C. vulgaris* cells. The addition of DCMU and DCBQ demonstrated that Q_B was not involved in photocurrent generation. Moreover, SPECM results indicate that electrons might originate from alternative electron pathways linked to PSI. A BPV device was assembled by coupling the proposed bioanode to a BOD-based biocathode which resulted in a considerable current density and power output for such microalgae-based devices. These results show boronic acid derivatives as promising element in tailoring bioanodes for microorganism-based BPV cells.

Declaration of Competing Interest

The authors declare the following financial interests/personal relationships which may be considered as potential competing interests: Z. Herrero-Medina reports financial support was provided by Rovira i Virgili University Department of Chemical Engineering. P. Wang reports financial support was provided by Ruhr University Bochum. Ioanis Katakis reports financial support was provided by Rovira i Virgili University Department of Chemical Engineering. Wolfgang Schuhmann reports financial support was provided by Ruhr University Bochum.

Acknowledgements

Z. Herrero-Medina acknowledges the support by a Marti Franquès scholarship of the Department of Chemical Engineering of the URV (Ref: 2018PMF-PIPF-27) and thanks Julio C. Zuaznabar-Gardona (now at CreatSens Health S.L.) for inspiring discussions. Part of this work was funded by a collaboration project between URV and King Abdulaziz University (contract number: TT16008). P. Wang is grateful for the financial support by the China Scholarship Council (CSC). A. Lielpetere is part of a project that has received funding from the European Union's Horizon 2020 research and innovation programme under grant agreement N°813006 (Implantsens).

Appendix A. Supplementary material

Supplementary data to this article can be found online at https://doi.org/10.1016/j.bioelechem.2022.108128.

References

[1] T.L. Chacón-Lee, G.E. González-Mariño, Microalgae for "healthy" foods-possibilities and challenges, Compr. Rev. Food Sci. Food Saf. 9 (2010) 655–675, https://doi.org/10.1111/j.1541-4337.2010.00132.x.

[2] R. Dineshlumar, R. Narendran, P. Jayasingam, P. Sampathkumar, Cultivation and chemical composition of microalgae Chlorella vulgaris and its antibacterial activity against human pathogens, J. Aquac. Mar. Biol. 5 (2017) 00119. https://doi.org/10.15406/jamb.2017.05.00119.

[3] R.G. de Melo, A.F. de Andrade, R.P. Bezerra, D.d.A. Viana Marques, V.A. da Silva, S.T. Paz, J.L. de Lima Filho, A.L.F. Porto, Hydrogel-based Chlorella vulgaris extracts: a new topical formulation for wound healing treatment, J. Appl. Phycol. 31 (6) (2019) 3653–3663, https://doi.org/10.1007/s10811-019-01837-2.

[4] I.T.K. Ru, Y.Y. Sung, M. Jusoh, M.E.A. Wahid, T. Nagappan, Chlorella vulgaris: a perspective on its potential for combining high biomass with high value bioproducts, Appl. Phycol. 1 (1) (2020) 2–11, https://doi.org/10.1080/26388081.2020.1715256.

[5] B. Ievina, F. Romagnoli, Potential of Chlorella species as feedstock for bioenergy production: A review, Environ. Clim. Technol. 24 (2020) 203–220, https://doi.org/10.2478/rtuect-2020-0067.

[6] P. Moradi, M. Saidi, Biodiesel production from Chlorella Vulgaris microalgal-derived oil via electrochemical and thermal processes, Fuel Process. Technol. 228 (2022) 107158, https://doi.org/10.1016/j.fuproc.2021.107158.

[7] E.S. Salama, J.H. Hwang, M.M. El-Dalatony, M.B. Kurade, A.N. Kabra, R.A.I. Abou-Shanab, K.H. Kim, I.S. Yang, S.P. Govindwar, S. Kim, B.H. Jeon, Enhancement of microalgal growth and biocomponent-based transformations for improved biofuel recovery: A review, Bioresour. Technol. 258 (2018) 365–375, https://doi.org/10.1016/j.biortech.2018.02.006.

[8] F.-L. Ng, S.-M. Phang, V. Periasamy, K. Yunus, A.C. Fisher, Enhancement of power output by using alginate immobilized algae in biophotovoltaic devices, Sci. Rep. 7 (2017) 16237, https://doi.org/10.1038/s41598-017-16530-y.

[9] R. Thorne, H. Hu, K. Schneider, P. Bombelli, A. Fisher, L.M. Peter, A. Dent, P. J. Cameron, Porous ceramic anode materials for photo-microbial fuel cells, J. Mater. Chem. 21 (2011) 18055–18060, https://doi.org/10.1039/c1jm13058g.

[10] C.-H. Thong, S.-M. Phang, F.-L. Ng, V. Periasamy, T.-C. Ling, K. Yunus, A.C. Fisher, Effect of different irradiance levels on bioelectricity generation from algal biophotovoltaic (BPV) devices, Energy Sci. Eng. 7 (5) (2019) 2086–2097, https://doi.org/10.1002/ese3.414.

[11] F.L. Ng, S.M. Phang, B.L. Lan, V. Kalavally, C.H. Thong, K.T. Chong, V. Periasamy, K. Chandrasekaran, G.G. Kumar, K. Yunus, A.C. Fisher, Optimised spectral effects of programmable LED arrays (PLA)s on bioelectricity generation from algal-biophotovoltaic devices, Sci. Rep. 10 (2020) 16105, https://doi.org/10.1038/s41598-020-72823-9.

[12] N. Sekar, Y. Umasankar, R.P. Ramasamy, Photocurrent generation by immobilized cyanobacteria via direct electron transport in photo-bioelectrochemical cells, Phys. Chem. Chem. Phys. 16 (2014) 7862–7871, https://doi.org/10.1039/c4cp00494a.

[13] L.T. Wey, P. Bombelli, X. Chen, J.M. Lawrence, C.M. Rabideau, S.J.L. Rowden, J. Z. Zhang, C.J. Howe, The development of biophotovoltaic systems for power generation and biological analysis, ChemElectroChem. 6 (21) (2019) 5375–5386, https://doi.org/10.1002/celc.201900997.

[14] R.A. Voloshin, V.D. Kreslavski, S.K. Zharmukhamedov, V.S. Bedbenov, S. Ramakrishna, S.I. Allakhverdiev, Photoelectrochemical cells based on photosynthetic systems : a review, Biofuel Res. J. 2 (2015) 227–235. https://doi.org/10.18331/BRJ2015.2.2.4.

[15] M. Anam, H.I. Gomes, G. Rivers, R.L. Gomes, R. Wildman, Evaluation of photoanode materials used in biophotovoltaic systems for renewable energy generation, Sustain, Energy Fuels. 5 (17) (2021) 4209–4232.

[16] A.J. McCormick, P. Bombelli, R.W. Bradley, R. Thorne, T. Wenzel, C.J. Howe, Biophotovoltaics: oxigenic photosynthetic organisms in the world of bioelectrochemical systems, Energy Environ. Sci. 8 (2015) 1092–1109, https://doi.org/10.1039/C4EE03875D.

[17] R.A. Bouhenni, G.J. Vora, J.C. Biffinger, S. Shirodkar, K. Brockman, R. Ray, P. Wu, B.J. Johnson, E.M. Biddle, M.J. Marshall, L.A. Fitzgerald, B.J. Little, J. K. Fredrickson, A.S. Beliaev, B.R. Ringeisen, D.A. Saffarini, The role of *Shewanella oneidensis* MR-1 outer surface structures in extracellular electron transfer, Electroanalysis 22 (2010) 856–864, https://doi.org/10.1002/elan.200880006.

[18] L.V. Richter, S.J. Sandler, R.M. Weis, Two isoforms of *Geobacter sulfurreducens* pilA have distinct roles in pilus biogenesis, cytochrome localization, extracellular electron transfer, and biofilm formation, J. Bacteriol. 194 (10) (2012) 2551–2563, https://doi.org/10.1128/JB.06366-11.

[19] J.Z. Zhang, P. Bombelli, K.P. Sokol, A. Fantuzzi, A.W. Rutherford, C.J. Howe, E. Reisner, Photoelectrochemistry of photosystem II in vitro vs in vivo, J. Am. Chem. Soc. 140 (1) (2018) 6–9, https://doi.org/10.1021/jacs.7b0856310.1021/jacs.7b08563.s001.

[20] K. Hasan, H. Bekir Yildiz, E. Sperling, P. Ó Conghaile, M.A. Packer, D. Leech, C. Hägerhäll, L.o. Gorton, Photo-electrochemical communication between cyanobacteria (Leptolyngbia sp.) and osmium redox polymer modified electrodes, Phys. Chem. Chem. Phys. 16 (45) (2014) 24676–24680.

[21] K. Hasan, E. Çevik, E. Sperling, M.A. Packer, D. Leech, L.o. Gorton, Photoelectrochemical wiring of *Paulschulzia pseudovolvox* (algae) to osmium polymer modified electrodes for harnessing solar energy, Adv. Energy Mater. 5 (22) (2015) 1501100, https://doi.org/10.1002/aenm.201501100.

[22] L. Darus, T. Sadakane, P. Ledezma, S. Tsujimura, I. Osadebe, D. Leech, L.o. Gorton, S. Freguia, Redox-polymers enable uninterrupted day/night photo-driven electricity generation in biophotovoltaic devices, J. Electrochem. Soc. 164 (3) (2017) H3037–H3040, https://doi.org/10.1149/2.0091703jes.

[23] H. Shkil, A. Schulte, D.A. Guschin, W. Schuhmann, Electron transfer between genetically modified Hansenula polymorpha yeast cells and electrode surfaces via Os-complex modified redox polymers, ChemPhysChem 12 (4) (2011) 806–813, https://doi.org/10.1002/cphc.201000889.

[24] G. Pankratova, L. Hederstedt, L. Gorton, Extracellular electron transfer features of Gram-positive bacteria, Anal. Chim. Acta. 1076 (2019) 32–47, https://doi.org/10.1016/j.aca.2019.05.007.

[25] A. Stephenson-Brown, S. Yong, M.H. Mansor, Z. Hussein, N.-C. Yip, P.M. Mendes, J. S. Fossey, F.J. Rawson, Electronic communication of cells with a surface mediated by boronic acid saccharide interactions, Chem. Commun. 51 (97) (2015) 17213–17216.

[26] M. Dervisevic, M. Senel, T. Sagir, S. Isik, Highly sensitive detection of cancer cells with an electrochemical cytosensor based on boronic acid functional polythiophene, Biosens. Bioelectron. 90 (2017) 6–12, https://doi.org/10.1016/j.bios.2016.10.100.

[27] X. Zhao, W. Deng, Y. Tan, Q. Xie, Promoting electricity generation of Shewanella putrefaciens in a microbial fuel cell by modification of porous poly(3-aminophenylboronic acid) film on carbon anode, Electrochim. Acta. 354 (2020) 136715, https://doi.org/10.1016/j.electacta.2020.136715.

[28] Z. Herrero-Medina, J.C. Zuaznabar-Gardona, I. Katakis, Photoelectrochemical communication of Chlorella vulgaris with poly (3-aminophenylboronic acid) modified electrodes. (2022) Submitted.

[29] J. Pruvost, G. Van Vooren, G. Cogne, J. Legrand, Investigation of biomass and lipids production with *Neochloris oleoabundans* in photobioreactor, Bioresour. Technol. 100 (23) (2009) 5988–5995, https://doi.org/10.1016/j.biortech.2009.06.004.

[30] F. Zhao, V. Hartmann, A. Ruff, M.M. Nowaczyk, M. Rögner, W. Schuhmann, F. Conzuelo, Unravelling electron transfer processes at photosystem 2 embedded in an Os-complex modified redox polymer, Electrochim. Acta. 290 (2018) 451–456, https://doi.org/10.1016/j.electacta.2018.09.093.

[31] F. Conzuelo, N. Marković, A. Ruff, W. Schuhmann, The open circuit voltage in biofuel cells: nernstian shift in pseudocapacitive electrodes, Angew. Chemie Int. Ed. 57 (41) (2018) 13681–13685, https://doi.org/10.1002/anie.201808450.

[32] R.J. Ritchie, Consistent sets of spectrophotometric chlorophyll equations for acetone, methanol and ethanol solvents, Photosynth. Res. 89 (1) (2006) 27–41, https://doi.org/10.1007/s11120-006-9065-9.

[33] F. Conzuelo, K. Sliozberg, R. Gutkowski, S. Grützke, M. Nebel, W. Schuhmann, High-resolution analysis of photoanodes for water splitting by means of scanning photoelectrochemical microscopy, Anal. Chem. 89 (2) (2017) 1222–1228, https://doi.org/10.1021/acs.analchem.6b03706.

[34] J. Szczesny, N. Marković, F. Conzuelo, S. Zacarias, I.A.C. Pereira, W. Lubitz, N. Plumeré, W. Schuhmann, A. Ruff, A gas breathing hydrogen/air biofuel cell comprising a redox polymer/hydrogenase-based bioanode, Nat. Commun. 9 (2018) 4715, https://doi.org/10.1038/s41467-018-07137-6.

[35] N. Azizi, M.R. Saidi, Highly chemoselective addition of amines to epoxides in water, Org. Lett. 7 (17) (2005) 3649–3651, https://doi.org/10.1021/ol051220q10.1021/ol051220q.s001.

[36] S. Bonollo, F. Fringuelli, F. Pizzo, L. Vaccaro, A green route to β-amino alcohols via the uncatalyzed aminolysis of 1,2-epoxides by alkyl- and arylamines, Green Chem. 8 (11) (2006) 960–964.
[37] S. Bonollo, D. Lanari, L. Vaccaro, Ring-opening of epoxides in water, European J. Org. Chem. 2011 (14) (2011) 2587–2598, https://doi.org/10.1002/ejoc.201001693.
[38] T. Kothe, S. Pöller, F. Zhao, P. Fortgang, M. Rögner, W. Schuhmann, N. Plumeré, Engineered electron-transfer chain in photosystem 1 based photocathodes outperforms electron-transfer rates in natural photosynthesis, Chem. - A Eur. J. 20 (35) (2014) 11029–11034, https://doi.org/10.1002/chem.201402585.
[39] K. Yokoyama, T. Shibasaki, Y. Murakami, Electrochemical characterization of enzyme electrodes mediated by ferrocene-containing acrylamide-acrylic acid copolymers, Denki Kagaku Oyobi Kogyo Butsuri, Kagaku. 64 (12) (1996) 1221–1227, https://doi.org/10.5796/kogyobutsurikagaku.64.1221.
[40] S. Koide, K. Yokoyama, Electrochemical characterization of an enzyme electrode based on a ferrocene-containing redox polymer, J. Electroanal. Chem. 468 (2) (1999) 193–201, https://doi.org/10.1016/S0022-0728(99)00174-6.
[41] A. Trebst, Inhibitors in the functional dissection of the photosynthetic electron transport system, Photosynth. Res. 92 (2) (2007) 217–224, https://doi.org/10.1007/s11120-007-9213-x.
[42] J. Tschörtner, B. Lai, J.O. Krömer, Biophotovoltaics: green power generation from sunlight and water, Front. Microbiol. 10 (2019) 866, https://doi.org/10.3389/fmicb.2019.00866.
[43] Y. Kashino, M. Yamashite, Y. Okamoto, H. Koike, K. Satoh, Mechanism of electron flow through the QB site in photosystem II. 3. Effects of the presence of membrane structure on the redox reactions at the QB site, Plant Cell Physiol. 37 (1996) 976–982, https://doi.org/10.1093/oxfordjournals.pcp.a029047.
[44] G. Ulas, G.W. Brudvig, Redirecting electron transfer in photosystem II from water to redox-active metal complexes, J. Am. Chem. Soc. 133 (34) (2011) 13260–13263, https://doi.org/10.1021/ja2049226.
[45] G. Saper, D. Kallmann, F. Conzuelo, F. Zhao, T.N. Tóth, V. Liveanu, S. Meir, J. Szymanski, A. Aharoni, W. Schuhmann, A. Rothschild, G. Schuster, N. Adir, Live cyanobacteria produce photocurrent and hydrogen using both the respiratory and photosynthetic systems, Nat. Commun. 9 (2018) 2168, https://doi.org/10.1038/s41467-018-04613-x.
[46] F. Zhao, S. Hardt, V. Hartmann, H. Zhang, M.M. Nowaczyk, M. Rögner, N. Plumeré, W. Schuhmann, F. Conzuelo, Light-induced formation of partially reduced oxygen species limits the lifetime of photosystem 1-based biocathodes, Nat. Commun. 9 (2018) 1973, https://doi.org/10.1038/s41467-018-04433-z.
[47] P. Cardol, G. Forti, G. Finazzi, Regulation of electron transport in microalgae, Biochim. Biophys. Acta. 1807 (8) (2011) 912–918, https://doi.org/10.1016/j.bbabio.2010.12.004.
[48] B. Bailleul, N. Berne, O. Murik, D. Petroutsos, J. Prihoda, A. Tanaka, V. Villanova, R. Bligny, S. Flori, D. Falconet, A. Krieger-Liszkay, S. Santabarbara, F. Rappaport, P. Joliot, L. Tirichine, P.G. Falkowski, P. Cardol, C. Bowler, G. Finazzi, Energetic coupling between plastids and mitochondria drives CO_2 assimilation in diatoms, Nature 524 (7565) (2015) 366–369, https://doi.org/10.1038/nature14599.
[49] V. Larosa, A. Meneghesso, N. La Rocca, J. Steinbeck, M. Hippler, I. Szabò, T. Morosinotto, Mitochondria affect photosynthetic electron transport and photosensitivity in a green alga, Plant Physiol. 176 (3) (2018) 2305–2314, https://doi.org/10.1104/pp.17.01249.
[50] C.B. Osmond, C.H. Foyer, G. Bock, M.R. Badger, S. von Caemmerer, S. Ruuska, H. Nakano, Electron flow to oxygen in higher plants and algae: rates and control of direct photoreduction (Mehler reaction) and rubisco oxygenase, Philos. Trans. R. Soc. London. B, Biol. Sci. 355 (1402) (2000) 1433–1446, https://doi.org/10.1098/rstb.2000.0704.
[51] D.F. Sueltemeyer, K. Klug, H.P. Fock, Effect of photon fluence rate on oxygen evolution and uptake by Chlamydomonas reinhardtii suspensions grown in ambient and CO2-enriched air, Plant Physiol. 81 (2) (1986) 372–375, https://doi.org/10.1104/pp.81.2.372.
[52] S. Upadhyaya, B.J. Rao, Reciprocal regulation of photosynthesis and mitochondrial respiration by TOR kinase in *Chlamydomonas reinhardtii*, Plant Direct. 3 (11) (2019), https://doi.org/10.1002/pld3.184.
[53] P. Wang, F. Zhao, A. Frank, S. Zerria, A. Lielpetere, A. Ruff, M.M. Nowaczyk, W. Schuhmann, F. Conzuelo, Rational design of a photosystem I photoanode for the fabrication of biophotovoltaic devices, Adv. Energy Mater. 11 (47) (2021) 2102858, https://doi.org/10.1002/aenm.202102858.
[54] M. Riedel, J. Wersig, A. Ruff, W. Schuhmann, A. Zouni, F. Lisdat, A Z-scheme-inspired photobioelectrochemical H_2O/O_2 cell with a 1 V open-circuit voltage combining photosystem II and PbS quantum dots, Angew. Chemie. Int. Ed. 58 (2019) 801–805, https://doi.org/10.1002/anie.201811172.
[55] X. Zhou, P. Gai, P. Zhang, H. Sun, F. Lv, L. Liu, S. Wang, Conjugated polymer enhanced photoelectric response of self-circulating photosynthetic bioelectrochemical cell, ACS Appl. Mater. Interfaces Interfaces. 11 (42) (2019) 38993–39000, https://doi.org/10.1021/acsami.9b12560.
[56] T. Adachi, K. Kataoka, Y. Kitazumi, O. Shirai, K. Kano, A bio-solar cell with thylakoid membranes and bilirubin oxidase, Chem. Lett. 48 (7) (2019) 686–689, https://doi.org/10.1246/cl.190176.